Variation of the Air Mass Exposure to Chlorophyll Over Eastern China Seas: an Insight into Marine Biogenic Aerosols

Shengqian Zhou[1], Ying Chen[1,2*], Fanghui Wang[1], Yang Bao[1], Xiping Ding[3]，Zongjun Xu[1]

[1]Shanghai Key Laboratory of Atmospheric Particle Pollution Prevention, Department of Environmental Science & Engineering, Institute of Atmospheric Sciences, Fudan University, Shanghai 200438, China.

[2]Institute of Eco-Chongming (IEC), Shanghai 202162, China.

[3]Pudong New District Environmental Monitoring Station, Shanghai 200135, China.

Corresponding author: Ying Chen (yingchen@fudan.edu.cn)

Key Points:

- Air mass exposure to chlorophyll (AEC) is a good indicator for the influence extent of marine biogenic emission on atmospheric environment
- Variation of AEC over the eastern Chin seas is co-controlled by surface chlorophyll *a* and boundary layer height
- AEC-based parameterization provides a new insight into simulating the distribution of marine biogenic aerosols

Abstract

Marine biological activities make substantial influences on aerosol composition and properties. The eastern China seas are highly productive with significant emissions of biogenic substances. Air mass exposure to chlorophyll *a* (AEC) can be used to indicate the influence of biogenic source on the atmosphere to a certain degree. In this study, the 12-year (2009–2020) daily AEC were calculated over the eastern China seas showing the spatial and seasonal patterns of marine biogenic influence intensity are co-controlled by surface phytoplankton biomass and boundary layer height. The AEC was linearly correlated with aerosol methanesulfonate (MSA) in each of three sub-regions, and the constructed parameterization scheme was applied to simulate the spatiotemporal variation of marine biogenic MSA. This AEC-based approach with observation constraints provides a new insight into the distribution of marine biogenic aerosols which may become increasingly important with the decline of terrestrial input to the studied region.

Plain Language Summary

Marine organisms can generate trace gases contributing to the formation and growth of atmospheric aerosols and thereby affect the climate. Along with the great reduction of air pollutants in China and weakening of East Asian winter monsoon, atmospheric transport of substances from mainland to the eastern China seas has declined significantly over the past decade. Accordingly, marine biogenic aerosols become increasingly important, which have not yet been well investigated. In this study, the air mass exposure to chlorophyll *a* (AEC) index representing the influence of marine biogenic source on the air was calculated over the eastern China seas during 2009 to 2020 based on air mass backward trajectories and surface chlorophyll retrieved from satellite images. The AEC values declined from the northwest to southeast region and were especially prosperous in spring, which was associated with the variations of surface chlorophyll *a* and boundary layer height. Taking aerosol methanesulfonate (MSA, a typically biogenic component) as a representative, we showed the capability of using the AEC and observations to simulate the variation of marine biogenic aerosol components. This method enables further exploration of the interaction between natural and anthropogenic aerosols and their environmental and climatic effects.

1 Introduction

Atmospheric aerosols, originating from numerous natural and anthropogenic sources, play critical roles in the Earth's climate system (Pöschl, 2005). Marine biological activities can produce and release a large quantity of organic compounds, which will make great contribution to marine aerosols via primary emissions in the form of sea spray aerosols and secondary formation of sea-to-air transferred gases (Carpenter et al., 2012; O'dowd et al., 2004). It has been estimated that the global emission of marine organic carbon (OC) aerosol was around 8 Tg $year^{-1}$, comparable to the magnitude of anthropogenic fossil and biofuel OC (Spracklen et al., 2008). The impact of marine biogenic source on aerosols often closely connects to the surface phytoplankton biomass (Mansour et al., 2020b; Rinaldi et al., 2013). For example, marine organic matters dominate the fine-mode aerosol mass during the blooming period and inorganic species are more important with the low-biological activities in the North Atlantic (O'dowd et al., 2004).

The eastern China seas (Bohai, Yellow and East China seas) are adjacent to densely populated eastern China, and the continental outflow of atmospheric pollutants may have notable

influence on aerosols over this region (Wang et al., 2016; Xu et al., 2021). Meanwhile, they are highly productive as a result of exogenous input of abundant nutrients, and the emissions of biogenic substances are much larger than oligotrophic seas (Zhang et al., 2014; Zhou et al., 2021). Several cruise and island based observations have shown the significance of marine biogenic source to carbonaceous aerosols (Kunwar and Kawamura, 2014; Li et al., 2022) and specific components (e.g. amines, carboxylic acids, sulfur-containing species) (Guo et al., 2016; Hu et al., 2015; Yang et al., 2009; Zhou et al., 2019). However, the spatiotemporal dynamics of marine biological influence on atmospheric environment and subsequent distributions of biogenic aerosol components are still poorly understood, due partly to the scarcity of field observation.

Air mass exposure to chlorophyll *a* (AEC), i.e. the weighted average concentration of sea surface chlorophyll *a* (Chl *a*) along the transport path of air mass, is a good surrogate for the extent to which the air mass at a specific site is affected by marine biogenic emissions (Arnold et al., 2010; Blazina et al., 2017; Park et al., 2018). This index encompasses (1) biogenic emission intensity proxied by surface Chl *a* concentration, (2) transport path characterized by air mass backward trajectory, and (3) diffusion and loss indicated by a weighting factor related to transport time. Zhou et al. (2021) have made improvement by adding a term reciprocal to boundary layer height (BLH), since BLH is a critical factor controlling ventilation and thereby concentrations of atmospheric components in the boundary layer. Based on this modified AEC index, the linkage between marine biogenic aerosol and phytoplankton biomass can be examined (Zhou et al., 2021). Aerosol methanesulfonate (MSA), as an important oxidation product of oceanic organism-derived dimethyl sulfide (DMS), is traditionally considered an indicator for marine biogenic sources (Park et al., 2017; Savoie et al., 2002; Yang et al., 2009). It is also one of the most abundant components of secondary organic aerosol (SOA) in marine environment (Facchini et al., 2008). Good correlations have been found between MSA and AEC in coastal seas when removing terrestrial perturbation and constraining air transport within marine boundary layer (MBL, (Zhou et al., 2021)).

In this study, based on air mass backward trajectories and satellite remote sensing products, we elucidated the spatiotemporal distribution of AEC over the eastern China seas during 2009 to 2020. These results showed how the influence extent of marine biogenic emission on MBL aerosols varies on a regional scale, which has not been addressed before. By integrating historical aerosol observations and AEC values, a parameterization scheme for the concentration of marine biogenic MSA is developed. The results demonstrate the prospect of estimating distribution of marine biogenic aerosols through an observation constrained method on the basis of AEC index. In the end, the potential rising importance of marine biogenic emissions compared to terrestrial transport was discussed by analyzing the decadal trend of terrestrial transport intensity.

2 Materials and Methods

2.1 Calculation of Trajectories and Relevant Indexes

The air mass backward trajectories were calculated by Hybrid Single-Particle Lagrangian Integrated Trajectories (HYSPLIT) model with input of Global Data Assimilation System (GDAS) Archived (1° × 1°) meteorology dataset. The starting height was 100 m and the

trajectory duration was 72 h. The BLH at each trajectory endpoint was extracted from GDAS dataset.

The AEC value for a specific trajectory was calculated by Equation 1:

$$AEC = \frac{\sum_{i=1}^{N_{total}} Chla_i \cdot e^{-\frac{t_i}{72} \cdot \frac{600}{BLH_i}}}{n} \quad (1)$$

where N_{total} is the total number of hourly endpoints (73 containing the receptor point) along the trajectory. $Chla_i$ represents the mean Chl *a* concentration (Terra-MODIS 8-day composite of Chl *a* concentration, 0.042° × 0.042°) within a radius of 20 km centered in the *i*th endpoint of a trajectory. t_i and BLH_i are the tracking time (hour) and BLH (m) of the *i*th endpoint, respectively. $e^{-\frac{t_i}{72}}$ is the weighting factor related to tracking time, because the location corresponding to longer transport time has weaker influence on the receptor site due to the diffusion and deposition along the transport. *n* is the number of endpoints with valid Chl *a* concentrations. The detailed calculation processes and associated data filtration rules refer to Zhou et al. (2021).

The air mass retention ratio over land (R_L), i.e. the weighted ratio of air transport time over land to the whole duration, was calculated by Equation 2 indicating the influence of terrestrial transport on the receptor site:

$$R_L = \frac{\sum_{i=1}^{N_{land}} e^{-\frac{t_i}{72}}}{\sum_{i=1}^{N_{total}} e^{-\frac{t_i}{72}}} \quad (2)$$

where N_{land} is the total number of trajectory endpoints located over land.

Based on aerosol observations during four cruises over the eastern China seas (Section 2.3 and Text S1), R_L index showed positive relationships with both typical anthropogenic metal Cd and dust-associated metal Al (Figure S1). The average concentrations of Cd and Al for $R_L >$ 0.75 were 5.8 and 14.5 times higher than for $R_L \leq 0.05$, respectively (medians were 23.6 and 16.6 times higher). These results presented the reasonability of using R_L as proxy for terrestrial transport.

In addition to AEC and R_L, the harmonic mean of BLH along trajectory (BLH_traj) and the retention ratio of air mass within MBL (R_{MBL}) were also calculated (Zhou et al., 2021).

2.2 Analysis of Spatiotemporal Variation

Our research domain (23−37° N, 117−130° E) includes the south Yellow Sea (YS), the East China Sea (ECS) and part of Northwest Pacific (NP). It was divided into 145 1° × 1° grids as shown in Figure S2. In order to reveal the spatiotemporal variations of AEC and R_L in this region, trajectories starting from the center of each grid were calculated with an interval of 6 hours during 1 January 2009 to 31 December 2020, and a total of 17532 trajectories were obtained for each grid. Then the R_L, AEC, BLH_traj (further divided to BLH_L and BLH_O for endpoints located over the land and ocean, respectively), R_{MBL} and AEC* (AEC index without the BLH term) indexes corresponding to each trajectory were calculated. Empirical orthogonal function (EOF) analysis, a widely used approach to extract the spatially and temporally varying modes from climate variables, was used to decompose the AEC and R_L monthly anomalies (144 × 145 matrixes). The principle and calculation method of EOF analysis can be found in Li et al. (2013).

2.3 Field Observations and Parameterization of Marine Biogenic MSA

Total suspended particulate (TSP) samples were collected by high-volume samplers in a total of 6 cruises in the eastern China seas during 2014 to 2020. The concentrations of water-soluble ions, including MSA, were determined by ion chromatography (IC) and trace metals were determined by inductively coupled plasma mass spectrometry (ICP-MS). The details about the cruise campaigns and aerosol measurements are given in Text S1 and Figure S3. Previously reported data of aerosol MSA from 2 islands (Huaniao Island 30.9° N, 122.7° E; and Okinawa Island 26.9° N, 128.2° E) and 8 cruise campaigns during 2009 to 2020 were also integrated for parameterization. The detailed locations, time periods, and data sources are listed in Table S1.

The entire research domain was split into three regions (Region 1 to Region 3) based on monthly averaged AEC dataset from 2009 to 2020 using the K-means clustering algorithm (shown in Figure 2b). The K-means clustering divide the initial dataset into a predefined number of subgroups by minimizing the sum of squared Euclidean distances between each data point and the corresponding cluster centers (Beddows et al., 2014). The data match-up between AEC and the concentration of marine biogenic MSA was performed for each region (see details in Text S2), and the linear regression functions between two variables were obtained. Using the parameterization scheme between MSA and AEC, the spatiotemporal distribution of marine biogenic MSA was simulated. For grids located on the boundary, the fitting parameters were obtained by linearly interpolating the parameters of two adjacent regions.

3 Results and Discussion

3.1 Spatiotemporal Distribution of AEC

According to previous study, the linkage between aerosol components and AEC could be established when marine air mass transported mainly within the boundary layer (Zhou et al., 2021). Therefore, the AEC and other indexes were filtrated by the condition of $R_{MBL} > 0.9$ in this study. The AEC generally decreased from the northwest to southeast oceanic regions with the highest values occurring in the majority of YS and coastal ECS in April and May, and the lowest indexes distributed in the NP especially in summer (Figure S4).

The EOF analysis of AEC showed that the first mode (Mode 1) could explain 77.3% of variance and decreased from the YS and northern coastal ECS to the remote ocean (Figure 1a). The corresponding principal component (PC1) demonstrated an annual cycle with the maximum in April and May and the minimum during November to January as well as an inter-annual variation with relatively high values in 2015–2017 (Figure 1b). Both spatial and seasonal variations of Mode 1 were co-controlled by surface Chl *a* and BLH. Specifically, higher values in the YS and coastal ECS generally accorded with higher Chl *a* concentrations and lower BLH (Figures S5–S7), and PC1 peaked in the late spring every year corresponding to almost each spike of Chl *a* (spring bloom) and trough of BLH (Figure 1b). The seasonal variation of BLH over the ECS was suggested to be affected by thermal stability defined as sea surface temperature minus the temperature at 850 hPa (Kuribayashi et al., 2011). The inter-annual variation of PC1 seemed predominantly driven by the BLH and its highest peaks in 2015–2017 were likely associated with the decreasing troughs of BLH during 2009 to 2016 and the increase afterwards (Figure 1b).

The second mode (Mode 2) explained 5.3% of overall variance. Its variation in the western YS and coastal ECS was opposite to the open ECS and NP (Figure 1a), which was likely caused by the distinct Chl *a* phenology in different regions. Due to the strong stratification limiting nutrient availability in the surface water and strong grazing pressure by microzooplankton (Guo et al., 2014; Liu et al., 2019), the concentration of surface Chl *a* in open ECS and NP reached the minimum in summer (Figure S5). But in coastal seas, the nutrient input from rivers and upwelling in summer sustained the phytoplankton biomass at a high level (Liu et al., 2019; Yamaguchi et al., 2013). Mode 2 dominated the seasonal variation of AEC in the remote ocean, and the time series of corresponding principle component (PC2) exhibited the minimum in summer (Figure 1b).

It should be noted that the highest Chl *a* along the coast especially in the outer Yangtze River Estuary is not reproduced by the distribution of AEC or AEC* (Figures S4–S6). It reflects the mismatch between local and air mass exposed Chl *a* concentrations. Accordingly, previous studies have indicated that variations of aerosol components cannot be linked to local surface Chl *a* synchronously and certain time lags exist for linking regional Chl *a* (Mansour et al., 2020a; Mansour et al., 2020b; Rinaldi et al., 2013). The AEC index, with more concrete characterization on the exposure of air mass to marine biogenic emission along air transport path, is likely to better connect with marine biogenic aerosols at the receptor site. Near-surface wind speed and sea surface temperature (SST), two factors affecting the sea-to-air fluxes of gases and sea spray aerosols (de Leeuw et al., 2011; Liss and Merlivat, 1986), are not considered in our AEC calculation. This may impact the abovementioned performance of AEC as an indicator for marine biological source. However, the effect of wind speed may be averaged out as obtaining the variation on a monthly resolution (Spracklen et al., 2008) and SST influence is much weaker than wind speed (Land et al., 2014; Li et al., 2019).

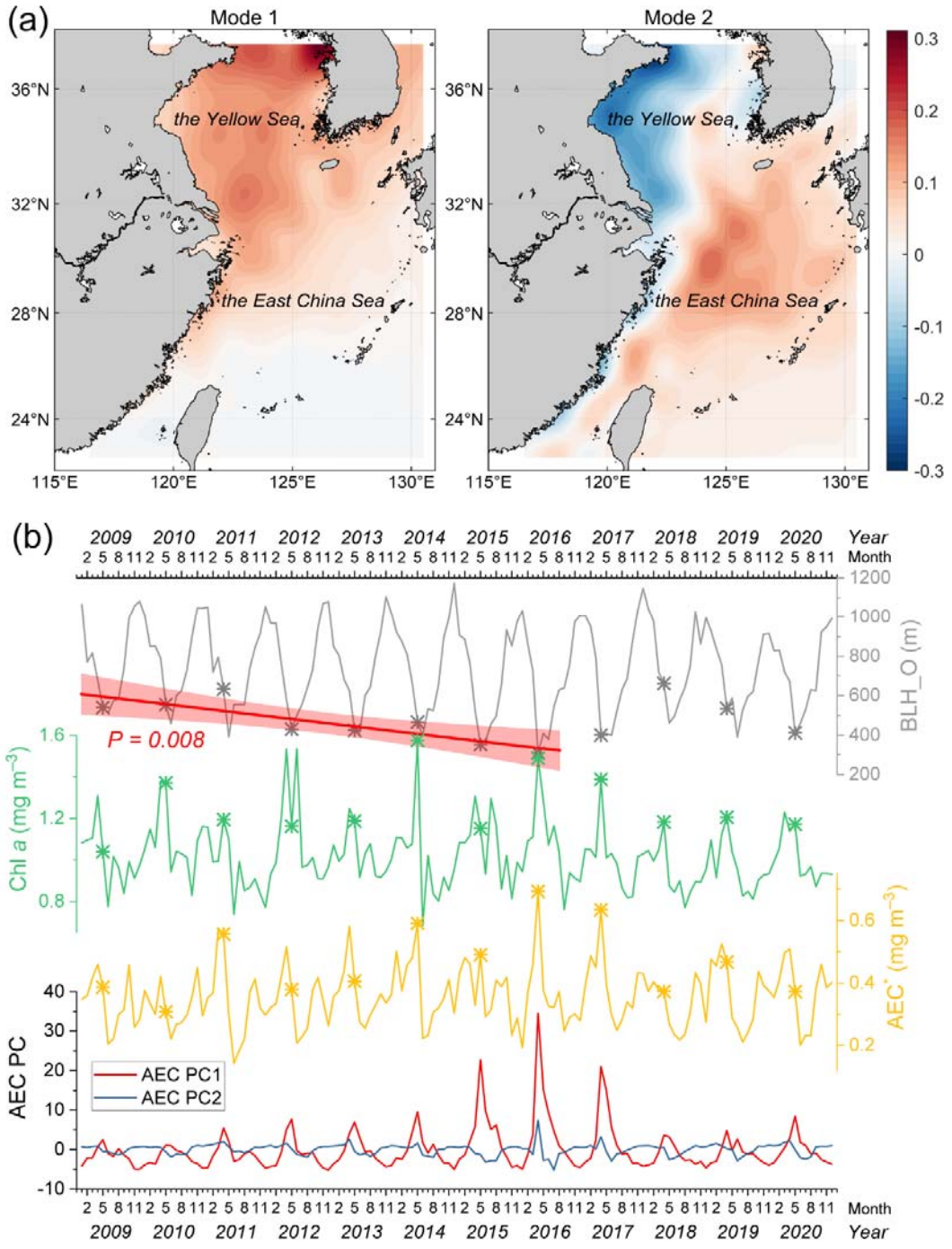

Figure 1. Spatiotemporal variation of air mass exposure to chlorophyll a (AEC) index and its controlling factors. (a) The first two EOF modes of AEC anomalies during 2009 to 2020. (b) Time series of principal components (PC) corresponding to the first teo EOF modes and monthly averages of AEC* value, Chl *a* concentration, and boundary layer height (BLH) along trajectories over the ocean (BLH_O) during 2009 to 2020. Note that AEC, AEC* and BLH_O were all filtrated by the condition of $R_{MBL} > 0.9$ (within marine boundary layer). The stars in series of AEC*, Chl *a*, and BLH_O correspond to the month in which the AEC PC1 reaches the

highest each year. The red line and shaded region in top panel represent the linear regression and corresponding 95% confidence interval for BLH_O at peak-AEC month between 2009 and 2016.

3.2 Simulation of Marine Biogenic MSA

Under the condition of $R_{MBL} > 0.9$, a significant correlation was found between aerosol MSA and the AEC index during the spring and summer but not in the autumn and winter over the eastern China seas (Figure S8). Correspondingly, MSA was not correlated with non-sea-salt SO_4^{2-} (nss-SO_4^{2-}) and the ratio of MSA to nss-SO_4^{2-} (MSA/nss-SO_4^{2-}) was significantly lower under high R_L regime than with low R_L during the spring and summer, while opposite phenomena existed in the autumn and winter (Figures S8–S9). This suggested that the conclusion drawn from the coastal island (MSA is dominantly from marine biogenic source in spring and summer but largely contributed by terrestrial transport in autumn and winter, (Zhou et al., 2021) might be applicable to the entire eastern China seas. Thus, the potential impacts of terrestrial MSA needs to be screened out when doing the data match-up (Text S2). Extremely low fraction of terrestrial air mass in summer (Figure 3a) and high biogenic emission in spring (Figure S4) can explain the dominance of biogenic MSA in these two seasons.

Considering the large spatial disparities in the variation and controls of AEC, and the emission rate of DMS related to phytoplankton community, temperature, radiation, mixed layer depth, etc. (Stefels et al., 2007; Vallina and Simó, 2007) from the coastal seas to open ocean, the research domain was divided into three regions by K-means clustering (Section 2.3.). The mean AEC value decreased from Region 1 to Region 3 with its peak time advancing from May to April (Figure S10). The seasonal variation of AEC in Region 1 was in accordance with marine biogenic MSA (filtrated by $R_L < 0.1$) over Huaniao Island, which was the highest in spring, followed by summer and then autumn and winter (Zhou et al., 2021). The seasonal change of AEC in Region 3 was consistent with the MSA observations over Okinawa Island and AEC PC2, showing the highest in spring and lowest in summer (Kunwar and Kawamura, 2014; Zhu et al., 2015). These results verified the feasibility of using AEC to infer the variation of marine biogenic MSA.

After data match-up and binning, good correlations were found between marine biogenic MSA and AEC for all three regions (Figure 2a). The linear fitting slope increased in the order of Region 1 < Region 2 < Region 3, which was opposite to the order of mean AEC. These linear regression functions could serve as a parameterization scheme for simulating the distribution of marine biogenic MSA between 2009 to 2020 (Figure 2b). It was found that the highest oceanic MSA concentrations appeared in April and May over Region 2, exceeding 0.1 μg m^{-3} (Figure 2b-c). According to historical observations, mean MSA concentration in spring over Region 1 (~ 0.050 μg m^{-3}) was lower than that over Region 2 (~ 0.065 μg m^{-3}), and this spatial characteristic was reproduced by the simulation. In summer, the MSA concentrations over the YS and coastal area (Region 1) were higher than other regions. However, in autumn and winter, the hot spot relocated to Region 3 probably due to high formation efficiency of aerosol MSA. Overall, the difference of marine biogenic MSA concentration among three regions was much lower than that of AEC value.

Four cruises during 2006 to 2007 over the northern YS (adjacent to Region 1) measured average MSA concentrations of 0.073, 0.039, 0.011, and 0.015 μg m^{-3} in spring (April – May), summer (July – August), autumn (October), and winter (January), respectively (Zhang and Yang, 2009; Zhang, 2009). The seasonal variation and concentration levels were similar to those of

simulated MSA in Region 1, except for slightly higher concentration in winter than in autumn likely associated with more terrestrial transport. MSA concentration over Jeju Island during 2001 to 2002 peaked in spring, with a seasonal mean of 0.066 μg m^{-3} similar to our estimates for Region 2 (0.074 μg m^{-3}) (Tyagi et al., 2017). The simulation of aerosol MSA over the eastern China seas by atmospheric chemical transport model (CTM) is scarce. Li et al. (2020) explored the atmospheric chemistry of oceanic DMS in this region via WRF-CMAQ model, but only the distribution of gas-phase MSA was provided, showing the highest in summer. The model did not incorporate aqueous-phase oxidation pathways, which could be the dominant mechanism of MSA formation (Hoffmann et al., 2016). As a result, large uncertainties may exist in the CTM simulating results. By contrast, our results inferred from the AEC index and constrained by observations could well capture the spatiotemporal distribution pattern of marine biogenic MSA in aerosols.

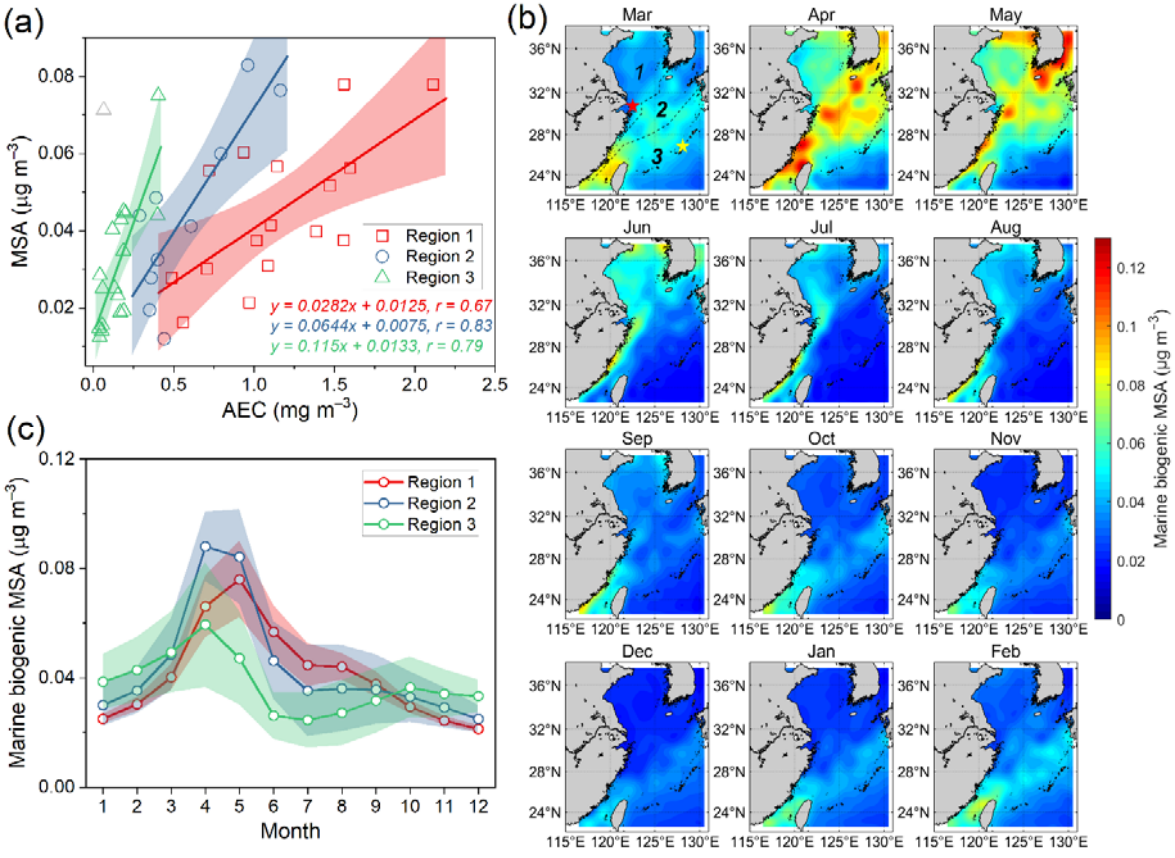

Figure 2. Parameterized simulation of spatiotemporal distribution of marine biogenic MSA. (a) Correlations between measured particulate MSA concentration and AEC index in each region. One data point of Region 3 (the gray triangle) was excluded from the correlation analysis. The shaded regions represent the 95% confidence interval of linear regression. (b) Monthly climatology of simulated marine biogenic MSA. Dashed lines show the boundaries among three regions. Red and yellow stars represent the location of Huaniao Island and Okinawa Island,

respectively. (c) The average concentrations of simulated marine biogenic MSA for each region in different months. The shaded band denotes the mean ± SD for each region.

3.3 Significance of marine biogenic source relative to terrestrial transport

Eastern China seas is significantly influenced by terrestrial transport, which may greatly weaken the relative importance of marine biogenic source to aerosols. The extent of terrestrial influence exhibited a decreasing trend from offshore to the remote ocean (YS > ECS > NP) and a significant seasonal variation (winter > spring and autumn > summer) (Figure 3a). The EOF analysis of R_L anomalies showed that Mode 1 explained 90.7% of total variance and exhibited identical signs over the entire studied region (Figure 3b), clearly showing the uniform control of East Asian monsoon. The R_L values over the ECS and NP were mostly below 0.1 in summer (Jun to August), suggesting extremely low terrestrial influence with prevailing southeast wind (Figure 1a). In this case, marine biogenic emission could be an important contributor to submicron organic aerosols and greatly affect radiative forcing.

As for winter, the intensity of terrestrial transport presented a significant decadal decrease (Figure 3c, $P < 0.05$) as the highest monthly mean and three-month (November, December, and January next year) mean of R_L during 2015 to 2020 dropped approximately 13.4% and 9.2% compared to the period of 2009 to 2014, respectively. This decadal decrease was likely caused by the weakening of East Asian winter monsoon after 1980s, influenced by large-scale climatic factors such as warming of NP (Pei et al., 2018), loss of Arctic sea-ice in autumn and extensive boreal snowfall in the earlier winter (Zou et al., 2017), variation of quasi-stationary planetary wave activity (Kang et al., 2009), and significant winter warming in northern China (Xu et al., 2006).

In the recent decade, China execute remarkable cut-down on air pollutant emissions. For example, SO_2 declined approximately 62% from 2010 to 2017 (Zheng et al., 2018) and thereby its outflow flux to the eastern China seas probably decreased by a larger fraction by integrating the change of R_L. Meanwhile, ship emission also dropped sharply due to the improvement of fuel oil quality with the establishment of Domestic Emission Control Areas and the implementation of "IMO 2020 regulation" (Yu et al., 2021; Zou et al., 2020). By contrast, no obvious decrease was found in the decadal changes of Chl *a* and AEC in the eastern China seas (Figure 1b), suggesting the elevated importance of marine biogenic source to aerosol components in this region (for example, sulfate and OC both related to MSA). For example, the MSA/nss-SO_4^{2-} during 2016–2018 was 1.4 times higher than that during 2013–2015 over Huaniao Island (Zhou et al., 2021). Considering the concurrent decline of terrestrial MSA, the ratio of biogenic MSA to nss-SO_4^{2-} was likely to exhibited a higher increase degree. Previous studies reported that average MSA/nss-SO_4^{2-} ratios over the eastern China seas were 0.00074 and 0.0038 in the winter of 2009 and summer of 2011, respectively (He et al., 2011; Zhang et al., 2014). Based on our cruise observations, the ratios reached 0.0057 and 0.018 in the winter of 2019 and summer of 2018, suggesting that fractional contribution of marine biogenic source to nss-SO_4^{2-} may have increased by over 5 times during this period.

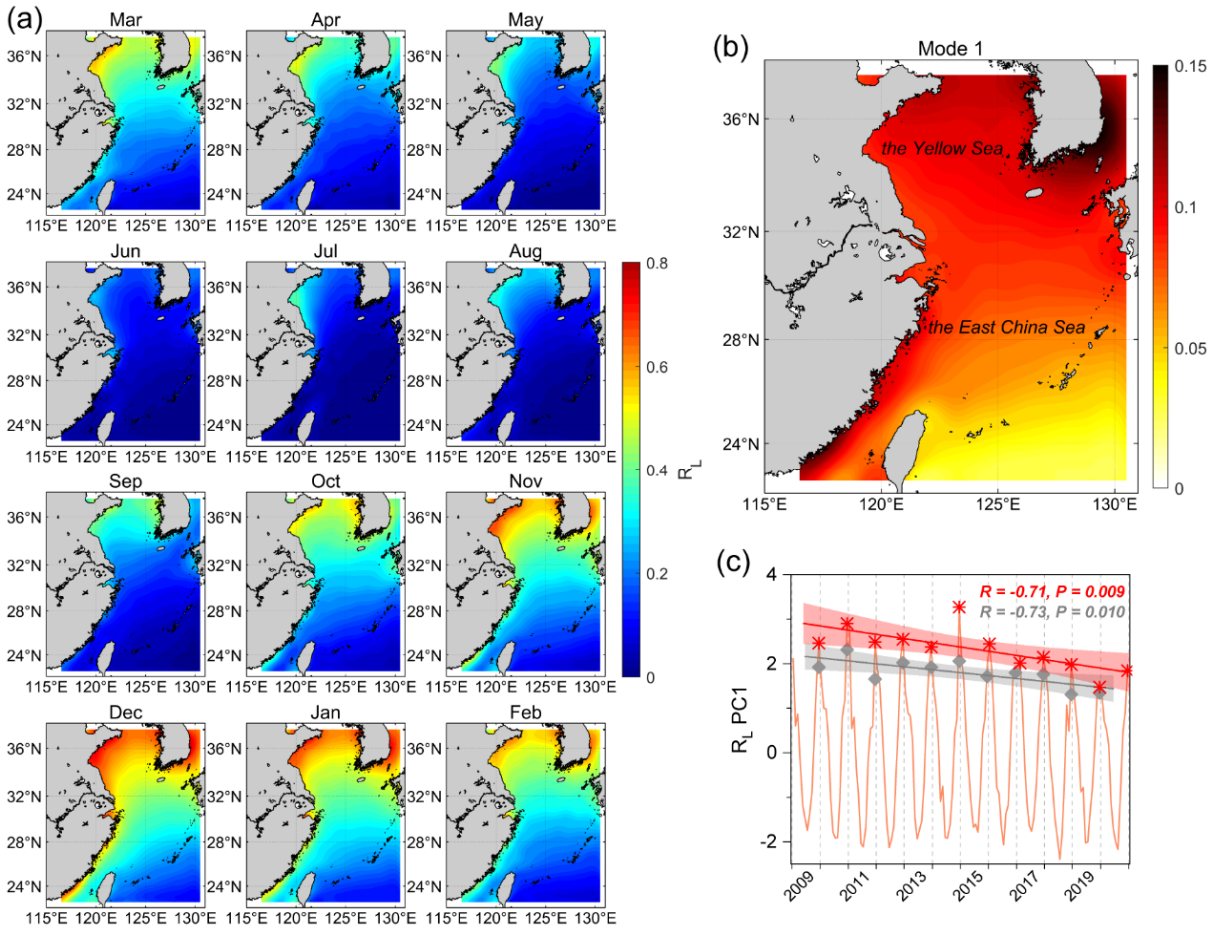

Figure 3. (a) Monthly climatology of R_L distribution during 2009–2020. (b) The first EOF mode of R_L monthly anomalies and (c) the time series of corresponding principal component (R_L PC1) during 2009–2020. The red star and gray diamond represent the highest monthly mean and the mean of November, December and January next year of R_L PC1, respectively. The linear lines and associated shaded bands show the linear regressions and their 95% confidence intervals.

4 Conclusions

Marine biogenic emissions from the eastern China seas may contribute significantly to atmospheric aerosols in spring and summer, and its fractional contribution exhibits a possibly decadal increase with the weakening of wintertime terrestrial transport and dramatic decrease of anthropogenic emissions. The AEC index quantifies how air masses are exposed to marine biogenic source during the transport. Using AEC as an indicator, this study investigates the 12-year spatiotemporal variations of the influence extent of marine biogenic emissions on boundary layer, which showed the highest in spring, and the lowest in winter for the YS and coastal ECS and in summer for the remote ocean, respectively. The spatial and seasonal patterns were co-controlled by surface phytoplankton biomass and BLH along the transport path, and the inter-annual change was predominantly associated with BLH.

The seasonal variations of calculated AEC value are generally consistent with measured MSA concentrations at the same region. By integrating aerosol MSA data observed on 14 cruises

and 2 islands, an AEC-based parameterization scheme was constructed and applied to simulate the spatiotemporal distribution of marine biogenic MSA. Although there are uncertainties in the empirical simulation results, this observation-constrained approach provides a different perspective for obtaining the distribution of biogenic sulfur in the atmosphere, particularly in the context that chemical mechanisms in CTMs are still less comprehensive (Li et al., 2020; Veres et al., 2020). Similar methods can also be applied to other marine biogenic components in the aerosol (Sanchez et al., 2021), especially for those relatively stable during the transport. The AEC calculation can also be improved by replacing Chl *a* concentration with other parameters more closely related to the aerosol component (e.g. sea surface DMS for biogenic sulfur aerosols) or adding other influencing factors like SST and radiation. Our study provides enlightenment on linking aerosol components and properties to marine biological activities and exploring the role of phytoplankton in potential ocean-aerosol-climate feedback with the perturbation of anthropogenic forcing.

Acknowledgments

We greatly thank the NOAA Air Resources Laboratory (ARL) for providing the HYSPLIT model, and NASA's OceanColor Web for the distribution of MODIS dataset. We acknowledge Dr. Rich Pawlowicz for developing and sharing the M_Map toolbox for Matlab, which was used in the mapping of this study. We also thank State Environmental Protection Key Laboratory of Ecological Management and System Regulation for Land-Sea Integration and National Observations and Research Station for Wetland Ecosystems of the Yangtze Estuary for their asistances in field observations. This work is jointly Sponsored by Natural Science Foundation of Shanghai (22ZR1403800), National Key Research and Development Program of China (2016YFA0601304), and National Key Basic Research Program of China (2014CB953701).

Open Research

The GDAS meteorological dataset can be accessed at ftp://ftp.arl.noaa.gov/pub/archives/gdas1. The remote-sensing Chl *a* datasets are available at https://oceandata.sci.gsfc.nasa.gov/. The aerosol measurement data during four 4 cruises (2017-2020) in the eastern China seas and corresponding indices (AEC, R_L, and R_{MBL}) are available at https://doi.org/10.5281/zenodo.7057317 (Zhou et al., 2022). Arranged data for constructing the parameterization scheme were listed in Table S1. All calculated 6-hour gridded data (AEC, AEC*, R_L, R_{MBL}, BLH_traj, BLH_L, BLH_O) and related Matlab code have been deposited in https://doi.org/10.5281/zenodo.7056981 (Zhou and Chen, 2022). The M_Map toolbox is publicly available at https://www.eoas.ubc.ca/~rich/map.html (Pawlowicz, 2020).

References

Arnold, S. R., Spracklen, D. V., Gebhardt, S., Custer, T., Williams, J., Peeken, I., and Alvain, S.

(2010), Relationships between atmospheric organic compounds and air-mass exposure to marine biology, *Environmental Chemistry*, *7*(3), 232-241, doi:10.1071/en09144.

Beddows, D. C. S., Dall'Osto, M., Harrison, R. M., Kulmala, M., Asmi, A., Wiedensohler, A., et al. (2014), Variations in tropospheric submicron particle size distributions across the European continent 2008–2009, *Atmospheric Chemistry and Physics*, *14*(8), 4327-4348, doi:10.5194/acp-14-4327-2014.

Blazina, T., Laderach, A., Jones, G. D., Sodemann, H., Wernli, H., Kirchner, J. W., and Winkel, L. H. (2017), Marine Primary Productivity as a Potential Indirect Source of Selenium and Other Trace Elements in Atmospheric Deposition, *Environmental Science & Technology*, *51*(1), 108-118, doi:10.1021/acs.est.6b03063.

Carpenter, L. J., Archer, S. D., and Beale, R. (2012), Ocean-atmosphere trace gas exchange, *Chemical Society Reviews*, *41*(19), 6473-6506, doi:10.1039/c2cs35121h.

de Leeuw, G., Andreas, E. L., Anguelova, M. D., Fairall, C. W., Lewis, E. R., O'Dowd, C., et al. (2011), Production flux of sea spray aerosol, *Reviews of Geophysics*, *49*(2), 2010RG000349, doi:10.1029/2010rg000349.

Facchini, M. C., Decesari, S., Rinaldi, M., Carbone, C., Finessi, E., Mircea, M., et al. (2008), Important source of marine secondary organic aerosol from biogenic amines, *Environmental Science & Technology*, *42*(24), 9116-9121, doi:10.1021/es8018385.

Guo, C., Liu, H., Zheng, L., Song, S., Chen, B., and Huang, B. (2014), Seasonal and spatial patterns of picophytoplankton growth, grazing and distribution in the East China Sea, *Biogeosciences*, *11*(7), 1847-1862, doi:10.5194/bg-11-1847-2014.

Guo, T., Li, K., Zhu, Y., Gao, H., and Yao, X. (2016), Concentration and size distribution of particulate oxalate in marine and coastal atmospheres – Implication for the increased importance of oxalate in nanometer atmospheric particles, *Atmospheric Environment*, *142*, 19-31, doi:10.1016/j.atmosenv.2016.07.026.

He, Y., Yang, G., and Zhang, H. (2011), Composition and source of atmosphere aerosol water soluble ions over the East China Sea in winter, *Environmental Science*, *32*(8), 2197-2203, doi:10.13227/j.hjkx.2011.08.034. *In Chinese*.

Hoffmann, E. H., Tilgner, A., Schroedner, R., Bräuer, P., Wolke, R., and Herrmann, H. (2016), An advanced modeling study on the impacts and atmospheric implications of multiphase dimethyl sulfide chemistry, *Proceedings of the National Academy of Sciences of the United States of America*, *113*(42), 11776-11781, doi:10.1073/pnas.1606320113.

Hu, Q., Yu, P., Zhu, Y., Li, K., Gao, H., and Yao, X. (2015), Concentration, Size Distribution, and Formation of Trimethylaminium and Dimethylaminium Ions in Atmospheric Particles over Marginal Seas of China, *Journal of the Atmospheric Sciences*, *72*(9), 3487-3498, doi:10.1175/jas-d-14-0393.1.

Kang, L., Chen, W., Gu, L., Huang, R., and Wang, L. (2009), Interdecadal Variations of the East Asian Winter Monsoon and Their Association with Quasi-Stationary Planetary Wave Activity, *Journal of Climate*, *22*(18), 4860-4872, doi:10.1175/2009jcli2973.1.

Kunwar, B., and Kawamura, K. (2014), One-year observations of carbonaceous and nitrogenous components and major ions in the aerosols from subtropical Okinawa Island, an outflow region of

418 Asian dusts, *Atmospheric Chemistry and Physics*, *14*(4), 1819-1836.

419 Kuribayashi, M., Ohara, T., and Shimizu, A. (2011), Temporal variation and vertical structure of
420 the marine atmospheric mixed layer over the East China Sea from Mie-scattering lidar data, *Sola*,
421 *7*, 189-192.

422 Land, P. E., Shutler, J. D., Bell, T. G., and Yang, M. (2014), Exploiting satellite earth observation
423 to quantify current global oceanic DMS flux and its future climate sensitivity, *Journal of*
424 *Geophysical Research: Oceans*, *119*(11), 7725-7740, doi:10.1002/2014jc010104.

425 Li, H., Qin, X., Wang, G., Xu, J., Wang, L., Lu, D., et al. (2022), Conjoint impacts of continental
426 outflows and marine sources on brown carbon in the East China sea: Abundances, optical
427 properties, and formation processes, *Atmospheric Environment*, *273*,
428 doi:10.1016/j.atmosenv.2022.118959.

429 Li, J., Carlson, B. E., and Lacis, A. A. (2013), Application of spectral analysis techniques in the
430 intercomparison of aerosol data: 1. An EOF approach to analyze the spatial-temporal variability of
431 aerosol optical depth using multiple remote sensing data sets, *Journal of Geophysical Research:*
432 *Atmospheres*, *118*(15), 8640-8648, doi:10.1002/jgrd.50686.

433 Li, S., Zhang, Y., Zhao, J., Sarwar, G., Zhou, S., Chen, Y., et al. (2020), Regional and Urban-Scale
434 Environmental Influences of Oceanic DMS Emissions over Coastal China Seas, *Atmosphere*, *11*(8),
435 doi:10.3390/atmos11080849.

436 Li, Y., He, Z., Yang, G.-P., Wang, H., and Zhuang, G.-C. (2019), Volatile halocarbons in the marine
437 atmosphere and surface seawater: Diurnal and spatial variations and influences of environmental
438 factors, *Atmospheric Environment*, *214*, 116820, doi:10.1016/j.atmosenv.2019.116820.

439 Liss, P. S., and Merlivat, L. (1986), Air-Sea Gas Exchange Rates: Introduction and Synthesis, *The*
440 *Role of Air-Sea Exchange in Geochemical Cycling*, *185*, 113-127.

441 Liu, X., Laws, E. A., Xie, Y., Wang, L., Lin, L., and Huang, B. (2019), Uncoupling of Seasonal
442 Variations Between Phytoplankton Chlorophyll a and Production in the East China Sea, *Journal*
443 *of Geophysical Research: Biogeosciences*, *124*(7), 2400-2415, doi:10.1029/2018jg004924.

444 Mansour, K., Decesari, S., Bellacicco, M., Marullo, S., Santoleri, R., Bonasoni, P., et al. (2020a),
445 Particulate methanesulfonic acid over the central Mediterranean Sea: Source region identification
446 and relationship with phytoplankton activity, *Atmospheric Research*, *237*, 104837,
447 doi:10.1016/j.atmosres.2019.104837.

448 Mansour, K., Decesari, S., Facchini, M. C., Belosi, F., Paglione, M., Sandrini, S., et al. (2020b),
449 Linking Marine Biological Activity to Aerosol Chemical Composition and Cloud‐Relevant
450 Properties Over the North Atlantic Ocean, *Journal of Geophysical Research: Atmospheres*,
451 *125*(13), e2019JD032246, doi:10.1029/2019jd032246.

452 O'dowd, C. D., Facchini, M. C., Cavalli, F., Ceburnis, D., Mircea, M., Decesari, S., et al. (2004),
453 Biogenically driven organic contribution to marine aerosol, *Nature*, *431*(7009), 676,
454 doi:10.1038/nature02959.

455 Park, K.-T., Jang, S., Lee, K., Yoon, Y. J., Kim, M.-S., Park, K., et al. (2017), Observational
456 evidence for the formation of DMS-derived aerosols during Arctic phytoplankton blooms,
457 *Atmospheric Chemistry and Physics*, *17*(15), 9665-9675, doi:10.5194/acp-17-9665-2017.

458 Park, K.-T., Lee, K., Kim, T.-W., Yoon, Y. J., Jang, E.-H., Jang, S., et al. (2018), Atmospheric DMS

in the Arctic Ocean and Its Relation to Phytoplankton Biomass, *Global Biogeochemical Cycles*, *32*(3), 351-359, doi:10.1002/2017gb005805.

Pawlowicz, R. (2020), M_Map: A mapping package for MATLAB (Version 1.4m) [Software]. https://www.eoas.ubc.ca/~rich/map.html.

Pei, L., Yan, Z., Sun, Z., Miao, S., and Yao, Y. (2018), Increasing persistent haze in Beijing: potential impacts of weakening East Asian winter monsoons associated with northwestern Pacific sea surface temperature trends, *Atmospheric Chemistry and Physics*, *18*(5), 3173-3183, doi:10.5194/acp-18-3173-2018.

Pöschl, U. (2005), Atmospheric aerosols: composition, transformation, climate and health effects, *Angewandte Chemie International Edtion in English*, *44*(46), 7520-7540, doi:10.1002/anie.200501122.

Rinaldi, M., Fuzzi, S., Decesari, S., Marullo, S., Santoleri, R., Provenzale, A., et al. (2013), Is chlorophyll-a the best surrogate for organic matter enrichment in submicron primary marine aerosol?, *Journal of Geophysical Research: Atmospheres*, *118*(10), 4964-4973, doi:10.1002/jgrd.50417.

Sanchez, K. J., Zhang, B., Liu, H., Saliba, G., Chen, C.-L., Lewis, S. L., et al. (2021), Linking marine phytoplankton emissions, meteorological processes, and downwind particle properties with FLEXPART, *Atmospheric Chemistry and Physics*, *21*(2), 831-851, doi:10.5194/acp-21-831-2021.

Savoie, D. L., Arimoto, R., Keene, W. C., Prospero, J. M., Duce, R. A., and Galloway, J. N. (2002), Marine biogenic and anthropogenic contributions to non-sea-salt sulfate in the marine boundary layer over the North Atlantic Ocean, *Journal of Geophysical Research*, *107*(D18), 4356, doi:10.1029/2001jd000970.

Spracklen, D. V., Arnold, S. R., Sciare, J., Carslaw, K. S., and Pio, C. (2008), Globally significant oceanic source of organic carbon aerosol, *Geophysical Research Letters*, *35*(12), L12811, doi:10.1029/2008gl033359.

Stefels, J., Steinke, M., Turner, S., Malin, G., and Belviso, S. (2007), Environmental constraints on the production and removal of the climatically active gas dimethylsulphide (DMS) and implications for ecosystem modelling, *Biogeochemistry*, *83*(1-3), 245-275, doi:10.1007/s10533-007-9091-5.

Tyagi, P., Kawamura, K., Kariya, T., Bikkina, S., Fu, P., and Lee, M. (2017), Tracing atmospheric transport of soil microorganisms and higher plant waxes in the East Asian outflow to the North Pacific Rim by using hydroxy fatty acids: Year-round observations at Gosan, Jeju Island, *Journal of Geophysical Research: Atmospheres*, *122*(7), 4112-4131, doi:10.1002/2016jd025496.

Vallina, S. M., and Simó, R. (2007), Strong relationship between DMS and the solar radiation dose over the global surface ocean, *Science*, *315*(5811), 506-508, doi:10.1126/science.1133680.

Veres, P. R., Neuman, J. A., Bertram, T. H., Assaf, E., Wolfe, G. M., Williamson, C. J., et al. (2020), Global airborne sampling reveals a previously unobserved dimethyl sulfide oxidation mechanism in the marine atmosphere, *Proceedings of the National Academy of Sciences of the United States of America*, *117*(9), 4505-4510, doi:10.1073/pnas.1919344117.

Wang, F., Chen, Y., Meng, X., Fu, J., and Wang, B. (2016), The contribution of anthropogenic sources to the aerosols over East China Sea, *Atmospheric Environment*, *127*, 22-33,

doi:10.1016/j.atmosenv.2015.12.002.

Xu, L., Liu, X. H., Gao, H. W., Yao, X. H., Zhang, D. Z., Bi, L., et al. (2021), Long-range transport of anthropogenic air pollutants into the marine air: insight into fine particle transport and chloride depletion on sea salts, *Atmospheric Chemistry and Physics*, *21*(23), 17715-17726, doi:10.5194/acp-21-17715-2021.

Xu, M., Chang, C.-P., Fu, C., Qi, Y., Robock, A., Robinson, D., and Zhang, H.-m. (2006), Steady decline of east Asian monsoon winds, 1969–2000: Evidence from direct ground measurements of wind speed, *Journal of Geophysical Research*, *111*(D24), D24111, doi:10.1029/2006jd007337.

Yamaguchi, H., Ishizaka, J., Siswanto, E., Baek Son, Y., Yoo, S., and Kiyomoto, Y. (2013), Seasonal and spring interannual variations in satellite-observed chlorophyll-a in the Yellow and East China Seas: New datasets with reduced interference from high concentration of resuspended sediment, *Continental Shelf Research*, *59*, 1-9, doi:10.1016/j.csr.2013.03.009.

Yang, G.-P., Zhang, H.-H., Su, L.-P., and Zhou, L.-M. (2009), Biogenic emission of dimethylsulfide (DMS) from the North Yellow Sea, China and its contribution to sulfate in aerosol during summer, *Atmospheric Environment*, *43*(13), 2196-2203, doi:10.1016/j.atmosenv.2009.01.011.

Yu, G., Zhang, Y., Yang, F., He, B., Zhang, C., Zou, Z., et al. (2021), Dynamic Ni/V Ratio in the Ship-Emitted Particles Driven by Multiphase Fuel Oil Regulations in Coastal China, *Environmental Science & Technology*, *55*(22), 15031-15039, doi:10.1021/acs.est.1c02612.

Zhang, H.-H., and Yang, G.-P. (2009), Biogenic emission of dimethylsulfide (DMS) from the North Yellow Sea and its contribution to non-sea-salt sulfate in aerosol, *Periodical of Ocean University of China*, *4*, 1672-5174. *In Chinese*.

Zhang, H. (2009), Stuides on Biogeochemistry of DMS and DMSP in the East China Sea and the Yellow Sea, PhD thesis, Ocean University of China. *In Chinese*.

Zhang, S. H., Yang, G. P., Zhang, H. H., and Yang, J. (2014), Spatial variation of biogenic sulfur in the south Yellow Sea and the East China Sea during summer and its contribution to atmospheric sulfate aerosol, *Science of the Total Environment*, *488-489*, 157-167, doi:10.1016/j.scitotenv.2014.04.074.

Zheng, B., Tong, D., Li, M., Liu, F., Hong, C., Geng, G., et al. (2018), Trends in China's anthropogenic emissions since 2010 as the consequence of clean air actions, *Atmospheric Chemistry and Physics*, *18*(19), 14095-14111, doi:10.5194/acp-18-14095-2018.

Zhou, S., and Chen, Y. (2022), Air mass exposure to chlorophyll a (AEC) over the eastern China seas (Version 1.0) [Dataset]. Zenodo. https://doi.org/10.5281/zenodo.7056981.

Zhou, S., Chen, Y., Paytan, A., Li, H., Wang, F., Zhu, Y., et al. (2021), Non‐Marine Sources Contribute to Aerosol Methanesulfonate Over Coastal Seas, *Journal of Geophysical Research: Atmospheres*, *126*(21), e2021JD034960, doi:10.1029/2021jd034960.

Zhou, S., Chen, Y., Wang, F., Bao, Y., Ding, X., and Xu, Z. (2022), Aerosol measurements over the eastern China seas during 2017 to 2020 [Dataset]. Zenodo. https://doi.org/10.5281/zenodo.7057317.

Zhou, S., Li, H., Yang, T., Chen, Y., Deng, C., Gao, Y., et al. (2019), Characteristics and sources of aerosol aminiums over the eastern coast of China: insights from the integrated observations in a

coastal city, adjacent island and surrounding marginal seas, *Atmospheric Chemistry and Physics*, *19*(16), 10447-10467, doi:10.5194/acp-19-10447-2019.

Zhu, C., Kawamura, K., and Kunwar, B. (2015), Organic tracers of primary biological aerosol particles at subtropical Okinawa Island in the western North Pacific Rim, *Journal of Geophysical Research: Atmospheres*, *120*(11), 5504-5523, doi:10.1002/2015jd023611.

Zou, Y., Wang, Y., Zhang, Y., and Koo, J. H. (2017), Arctic sea ice, Eurasia snow, and extreme winter haze in China, *Science Advances*, *3*(3), e1602751, doi:10.1126/sciadv.1602751.

Zou, Z., Zhao, J., Zhang, C., Zhang, Y., Yang, X., Chen, J., et al. (2020), Effects of cleaner ship fuels on air quality and implications for future policy: A case study of Chongming Ecological Island in China, *Journal of Cleaner Production*, *267*, doi:10.1016/j.jclepro.2020.122088.

References From the Supporting Information

Fu, J., B. Wang, Y. Chen, and Q. Ma (2018), The influence of continental air masses on the aerosols and nutrients deposition over the western North Pacific, *Atmospheric Environment*, *172*, 1-11, doi:10.1016/j.atmosenv.2017.10.041.

He, Y. (2011), Composition and Sorce of Atmosphere Aerosol Water Soluble Ions over the China Coastal Seas, Master thesis, Ocean University of China. *In Chinese*.

Ji, J., L. Chen, J. Wang, H. Lin, and Q. Lin (2016), Characters of the aerosol over the northwest Pacific and eastern China coastal area in autumn, *Journal of Applied Oceanography*, *35*(3), 339-347, doi:10.3969/J.ISSN.2095-4972.2016.03.004. *In Chinese*.

Pilson, M. E. (2012), *An Introduction to the Chemistry of the Sea*, Cambridge University Press.

Xue, L. (2012), Temporal-spatial Variations and Chemical Characteristics of Atmospheric Aerosol over the East China Marginal Seas, Master thesis, Ocean University of China. *In Chinese*.

Yang, T., Y. Chen, S. Zhou, H. Li, F. Wang, and Y. Zhu (2020), Solubilities and deposition fluxes of atmospheric Fe and Cu over the Northwest Pacific and its marginal seas, *Atmospheric Environment*, *239*, 117763, doi:10.1016/j.atmosenv.2020.117763.

Zhang, S. H., G. P. Yang, H. H. Zhang, and J. Yang (2014), Spatial variation of biogenic sulfur in the south Yellow Sea and the East China Sea during summer and its contribution to atmospheric sulfate aerosol, *Science of the Total Environment*, *488-489*, 157-167, doi:10.1016/j.scitotenv.2014.04.074.

Zhou, S.-j., H.-h. Zhang, and G.-p. Yang (2018), Distributions and chemical characteristics of water soluble ions in PM2.5 and PM10 over the East China Sea, *China Environmental Science*, *38*(3), 900-909, doi:10.19674/j.cnki.issn1000-6923.2018.0104. *In Chinese*.

Zhou, S., Y. Chen, A. Paytan, H. Li, F. Wang, Y. Zhu, T. Yang, Y. Zhang, and R. Zhang (2021), Non‐Marine Sources Contribute to Aerosol Methanesulfonate Over Coastal Seas, *Journal of Geophysical Research: Atmospheres*, *126*(21), e2021JD034960, doi:10.1029/2021jd034960.

Zhu, C., K. Kawamura, and B. Kunwar (2015), Organic tracers of primary biological aerosol particles at subtropical Okinawa Island in the western North Pacific Rim, *Journal of Geophysical Research: Atmospheres*, *120*(11), 5504-5523, doi:10.1002/2015jd023611.